Observation of the Alpha Particle "Knock-On" Neutron Emission from Magnetically Confined DT Fusion Plasmas

J. Källne, L. Ballabio, J. Frenje, S. Conroy, G. Ericsson, M. Tardocchi, and E. Traneus
Department of Neutron Research, Uppsala University, EURATOM-NFR Association, Uppsala, Sweden

G. Gorini
INFM, Physics Department, Milano–Bicocca University, and Plasma Physics Institute, EURATOM-ENEA-CNR Association, Milano, Italy

(Received 27 January 2000)

Suprathermal fuel ions from α-particle knock-on collisions in fusion DT plasmas are predicted to cause a weak feature in the neutron spectrum of $d + t \rightarrow \alpha + n$. The knock-on feature has been searched for in the neutron emission of high (>1 MW) fusion-power plasmas produced at JET and was found using a magnetic proton recoil type neutron spectrometer of high performance. Measurement and predictions agree both in absolute amplitude and in plasma-parameter dependence, supporting the interpretation and model. Moreover, the results provide input to projecting α-particle diagnostics for future self-heated fusion plasmas.

PACS numbers: 52.55.Pi, 28.52.–s, 52.55.Fa, 52.70.Nc

Thermonuclear ignition in deuterium-tritium (DT) fusion plasmas requires that 3.5-MeV α particles from the reaction $d + t \rightarrow \alpha + n$ are effectively thermalized to provide maximum self-heating. In tokamaks, the thermalization time is of the order of $\tau \approx 1$ s during which the fast α particles must be well contained. The physics of fast α particles is a central topic in high-power DT plasma studies, and experiments in this field are now becoming possible. Dedicated detection techniques are needed for the α-particle diagnosis of the present DT experiments, and several concepts have been proposed such as those where the confined $^4He^{+2}$ ions are singly or doubly neutralized by injecting a deuteron beam or lithium pellet resulting in observation of characteristic light emission [1] from He^{+1} or neutral ^4He emission [2]. The approach reported here is based on neutron emission spectroscopy measurements.

As first suggested [3], and quantitatively predicted in [4–7], the fast α-particle population creates a suprathermal component of fuel ions through knock-on collisions. Reactions involving these fuel ions create a weak high-energy tail in the neutron emission spectrum at 1.5 MeV above the peak at $E_n \approx 14$ MeV. This is referred to as the alpha-particle knock-on neutron (AKN) emission in contrast to the normal deuteron-triton neutron (DTN) emission. Detection of the AKN feature requires a powerful neutron spectrometer viewing a plasma of sufficient fusion energy E_f, i.e., fusion power (P_f) times pulse length (t_p). The limit for detecting the AKN effect was surpassed when the Joint European Torus (JET) in 1997 produced DT discharges of record high fusion energy [8] which were observed with a new neutron spectrometer of the MPR (magnetic proton recoil) type [9]. Here, we report on the first observation of the AKN emission, compare it with theoretical predictions, and discuss the implications for the use of neutron spectrometry as an α-particle diagnostic on the next step tokamak experiments aiming for ignition.

The first main DT experiment at JET (DTE1) has produced a number of high-power discharges with $P_f \geq 1$ MW (and corresponding neutron, or α-particle, yield rates of $Y_n > 5 \times 10^{17}$ n/s) for periods of $t_p \leq 4$ s. These conditions were reached using NB (neutral beams, producing up to 20 MW) and rf (radio frequency wave) heating. Both create a suprathermal fuel ion population, but the one related to NB extends no further than the beam energy (about 150 keV) which is not high enough to interfere with the observation of the AKN emission; this is not true for rf. A series of twelve NB discharges chosen for this study had a maximum yield rate of $Y_n \approx 4 \times 10^{18}$ n/s giving an MPR count rate of $C_n \approx 4 \times 10^5$ n/s, i.e., a C_n/Y_n ratio of 10^{-13}. The total neutron yield of this series was 3×10^{19} so the MPR data base consists of 3×10^6 events. The spectral region of observation (RO, see below) is limited to the high energy tail of 150 events, i.e., the average event fraction is $R_{RO} \approx 5 \times 10^{-5}$. This data set is about the minimum that permits differentiation with respect to neutron energy (E_n) and discharges of different conditions (especially, electron temperature T_e) which is required for a positive identification of the AKN emission.

The AKN emission is a three-step process that starts with a $d + t \rightarrow \alpha + n$ reaction, proceeds by an α-particle knock-on collision ($\alpha + d \rightarrow \alpha + d'$ or $\alpha + t \rightarrow \alpha + t'$) and ends with $d' + t \rightarrow \alpha + n$ or $t' + d \rightarrow \alpha + n$; here d' and t' indicate fuel ions of the suprathermal knock-on population extending up to $E_{d'} \approx 3.2$ MeV and $E_{t'} \approx 3.5$ MeV. The shape of the AKN spectrum is known from calculations [7] as is the amplitude relative to the main DTN emission as a function of pertinent plasma conditions. The DTN emission is here taken as a superposition of DTNi (due to the bulk population of isotropic fuel ions) and DTNa (due to the anisotropic population directly related to the NB injection

 0031-9007/00/85(6)/1246(4)$15.00

[10]). A third potential contribution is the emission of triton burnup neutrons (TBN) where the primary reaction is $d + d \rightarrow t' + p$ (i.e., the parallel branch to $d + d \rightarrow {}^3\mathrm{He} + n$ referred to as DDN emission) forming a suprathermal t' population extending up to $E_{t'} \approx 1$ Me; the shape and amplitude (relative to DDN) of TBN are well known from calculations and measurements [11]. The TBN and AKN processes both involve nuclear burnup of a fast fuel ion whose rates, relative to DDN and DTN, respectively, increase with the slowing down time and, hence, T_e ($\tau \propto T_e^{3/2}$). The AKN process involves α-particle slowing down as well so it varies as $\tau \propto T_e^{\kappa}$, with $\kappa \approx 3$ [7] thus distinguishing it from TBN ($\tau_\alpha \approx \tau_{t'} \leq 1$ s for JET plasmas).

Spectra of AKN and DTN emission were calculated (Fig. 1) and folded with the MPR response function that specifies the relationship between the energy distribution of the incoming neutron flux and the proton recoil position distribution recorded, $I_p(X)$ (see below). The thus calculated $I_p(X)$ histogram was fitted to the data and the parametrized source functions were determined through a minimization procedure. The DTNi spectrum was taken to be Gaussian (variable width, Γ_G) while DTNa and AKN spectra were of fixed shape (as calculated for reference plasma conditions). All components had variable amplitudes and were fixed in energy but for a general shift ΔE_S to account for plasma toroidal rotation [12]. These results were used to calculate the energy integrated emission ratio AKN/DTN and the intensity ratio $R_{\mathrm{AKN}} =$ AKN(RO)/DTN where AKN(RO) is introduced to permit practical comparison with the measured quantity, R_{RO}; RO is defined to start at the intersection of the AKN and DTNi curves ($E_n = 15.5$ MeV in Fig. 1). Similarly, the ratio $R_{\mathrm{TBN}} =$ TBN(RO)/DTN was calculated to predict the TBN interference. The calculations were performed for each discharge considering relevant plasma conditions; for the purposes of this study, time averaged values for the plasma core were used as derived from the JET diagnostic data base.

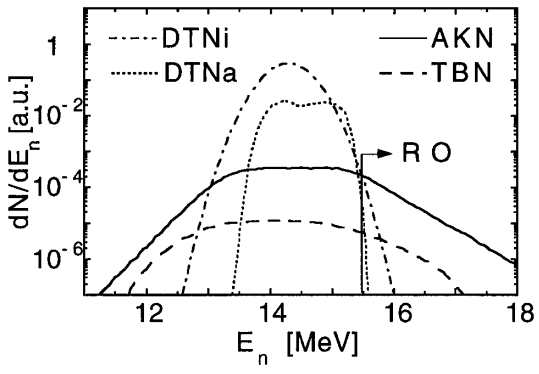

FIG. 1. Results on calculated spectra of the AKN, DTNi, and DTNa emission components describing data (see text); the TBN emission is shown for comparison. RO indicates the region for observing AKN and determining the ratio R_{AKN}.

The MPR neutron spectrometer [9] consists, in short, of a neutron collimator ending with a polythene target foil where part ($\approx 10^{-6}$) of the incoming neutron flux is converted to a proton recoil flux whose energy distribution is measured as the momentum dispersed position distribution, $I_p(X)$. The neutron flux detection efficiency is $\varepsilon = 1.2 \cdot 10^{-4}$ cm^2 at an energy resolution of $\Delta E_n/E =$ 4% (FWHM). The total event rate was up to near 10^6 s^{-1} in which case the RO event rate was at the level of 10^1 s^{-1}. The distribution $I_p(X)$ is measured with a scintillator hodoscope (36 active channels) so the result is a position histogram of count rates (Fig. 2), recorded in scalers that were read every 10 ms. In addition, pulse heights were recorded for the purpose of identifying signal events and to determine the background admixture relative to the signal (the ratio B/S) in the scaler data which was appropriately corrected for. For instance, the recorded pulse height spectra for the first hodoscope channel in the RO range (Fig. 3) shows a clear signal event peak for a plasma of $T_e \approx 8.6$ keV, while it is much suppressed for a plasma of low T_e (4 keV). This B/S difference is expected if the signal events are due AKN while, for instance, fortuitous pileup cannot be the explanation as the detector event rates are similar. The rest of the pulse height spectrum is described with a fitted analytical function which was used to determine the correction factor applied to the raw $I_p(X)$ data; the correction was significant for channel numbers $\geq$29 including numbers 31 to 35 of RO (the range $X = 400$–500 mm).

The best example of measured position histograms is shown in Fig. 2. Here one can see a high-energy slope with an inflection point at $X \approx 400$ mm where the amplitude is down by 4 orders of magnitude. The experimental results are compared with model calculations based on the two aforementioned DTN components (plus a low-energy neutron scattering background), besides the searched for AKN component. The model is parametrized with respect

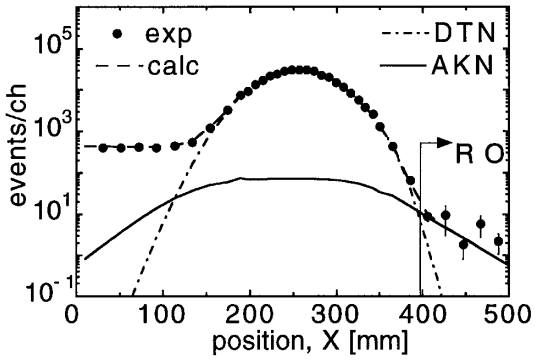

FIG. 2. Example of a measured recoil position histogram and the results of calculated contributions from the DTN and AKN emission besides a scattered neutron background for $X < 150$ mm. The energy dispersion is $\Delta E_n/\Delta x \approx +10$ keV/mm at a resolution of 4%. The channel width is 8.5 mm in the center (used to present the data) and 20.5 mm in the wings.

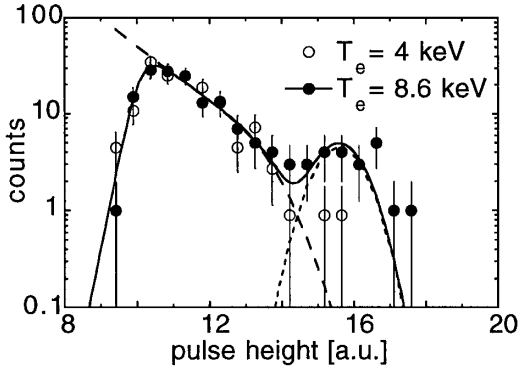

FIG. 3. Pulse height spectra for the hodoscope channel No. 31 for plasmas of different electron temperature (T_e). The T_e = 8.6 keV data are fitted (full line) with an analytical function of signal (dotted) and background (dashed) components.

to amplitudes besides the width Γ_G representing the DTNi emission; Γ_G is taken as due to thermal Doppler broadening with an apparent ion temperature T_i. The measurement is well accounted for (with $\chi^2 \approx 2$) by the model. It shows that the neutron emission is dominated by the DTNi component peaking at $E_n \approx 14.3$ MeV (Fig. 1) with a high-energy slope out to $E_n \approx 15.2$ MeV where the DTNa component shows up as a local enhancement at 15.2 MeV. The conspicuous break in the slope at $X = 400$ of Fig. 2 is of another origin such as AKN emission. The TBN emission can produce a high-energy tail but is predicted (Fig. 1) to be weaker than AKN and of shorter extension ($E_n \leq 18$ MeV). The AKN and TBN shape difference is rather independent of plasma conditions [7] so it would be the feature to use to distinguish them experimentally given data extending beyond $E_n \approx 17$ MeV. This is not the case here so one has to go by the predicted relative amplitude $R_{\mathrm{TBN}}/R_{\mathrm{AKN}}$. Thus, the tail in Fig. 2 should be ascribed to AKN emission as it is stronger by an order of magnitude.

The measured relative event rate in the AKN dominated region RO varies between the discharges studied which is examined in Fig. 4 as a function of electron temperature in the range $T_e = 4$ to 9 keV. The data show a T_e dependence that is consistent with the theoretically predicted power law scaling $R_{\mathrm{RO}}(T_e) = T_e^{\kappa}$ where $\kappa = 3.2$ [7] and provides a better description of observation than does one based on TBN with $\kappa = \frac{3}{2}$. This is thus supporting evidence of interpreting the RO events as due to AKN emission.

For the discharges studied, the triton concentration c_t, given as the density ratio $c_t = n_t/(n_d + n_t)$, was varied in the range $c_t = 30\%$ to $c_t = 90\%$. This, besides the T_e dependence over the range 4 to 9 keV, affects both the R_{AKN} value and the degree of the potential interference from the TBN emission [7]. The predicted R_{AKN} variation is large (a factor of 7) and the $R_{\mathrm{TBN}}/R_{\mathrm{AKN}}$ ratio is small (on the scale of the experimental error in R_{RO}), but for the case of the lowest tritium concentration ($c_t = 30\%$); for this case, TBN would contribute 34% to R_{RO} so a reduced value of $R_{\mathrm{RO}} = 8.4 \pm 3.6) \times 10^{-5}$ was determined. It is found that the AKN prediction indeed describes the variation in experimental results on R_{RO} within the statistical errors (Fig. 5); the systematic errors are estimated to be smaller, at the 10% to 20% level, partly due to the DTN contribution to R_{RO} (cf. Fig. 1) besides the uncertainties in the calculations from the diagnostic information input used. The agreement between measurement and the calculations, including the plasma condition dependencies in both T_e and c_t, thus provides additional positive identification of the AKN emission in the data. Previously, the α-particle population in JET DT discharges has been inferred from the augmented heating due to α particles as evidenced in the observation of an increase in T_e with P_f [13].

The predicted T_e dependence in the AKN/DTN ratio and the AKN spectral shape, combined with the empirical normalization using the data on the AKN emission for the limited spectral region RO, can be used to project the AKN emission fraction for a wide T_e range (Fig. 6). This shows that the AKN emission fraction increases rapidly

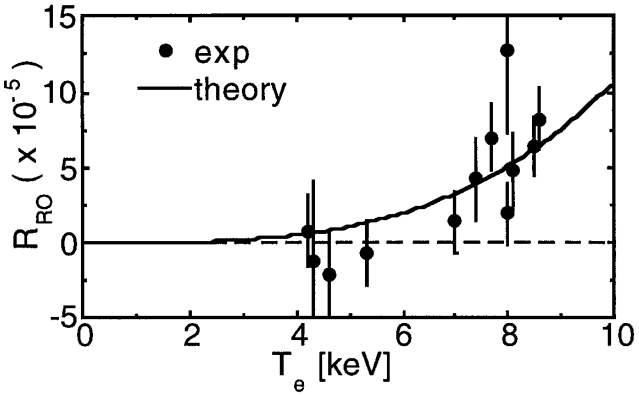

FIG. 4. Measured relative neutron emission over the region of interest (R_{RO}) for 12 plasma discharges of different T_e with fitted power function, $R_{\mathrm{RO}} \propto T_e^{\kappa}$ ($\kappa = 3.2$). The error bars are statistical and include background subtraction contributions.

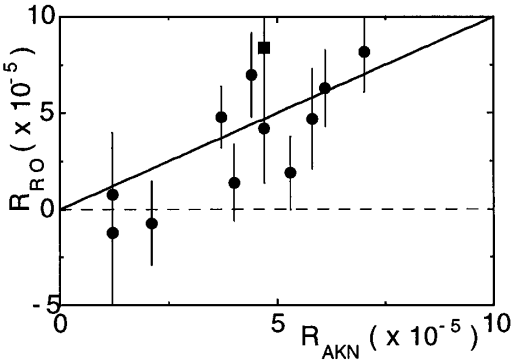

FIG. 5. Measured (R_{RO}) vs predicted (R_{AKN}) relative neutron emissions over the region of observation. The square indicates the R_{RO} value before correction for TBN contribution. The line indicates $R_{\mathrm{RO}} = R_{\mathrm{AKN}}$.

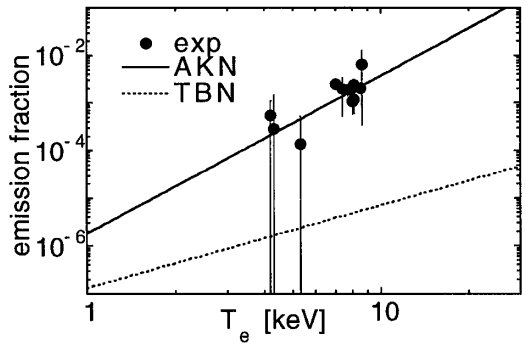

FIG. 6. The AKN fraction of the neutron emission derived from the data of Fig. 4 as function electron temperature compared to the theoretical functional dependence which is also shown for the TBN fractional emission.

with T_e under diminishing TBN interference (a factor 20 in going from the JET conditions of $T_e \geq 4$ keV to the expected burning plasma regime of $T_e > 20$ keV; T_e is the single most important plasma parameter, so this sets the framework for AKN measurements.

The AKN calculation assumes classical fast ion confinement and involves a detailed determination of the $\alpha + t$ and $\alpha + d$ scattering in the energy range $E < 4$ MeV [7]. This study represents the first empirical test of the applicability of the AKN model. The found agreement between the measured and predicted AKN emission is thus consistent with other observations [14] that fast particle confinement in JET plasmas does not deviate from the classical limit under normal conditions. Alternatively, assuming that the classical confinement applies, the AKN prediction is confirmed through the present study. However, to perform quantitative studies of this kind requires data of some 10× better statistics which would also be the qualifier for AKN as an α-particle diagnostic and certain to be met in future experiments on burning fusion plasmas. The main parameters affecting the AKN measurements would change as follows if comparing present JET and ITER types of plasmas [15]: $T_e(9 \rightarrow 20$ keV), $P_f(10$ MW $\rightarrow 1$ GW), and $t_p(1 \rightarrow 10^3$ s). This means that the AKN emission would be observed with a factor of 10^4 better statistics from increased count rate due to higher P_f and AKN/DTN emission ratio (see Fig. 6) besides the use of longer data integration time (as 10 s would provide sufficient time resolution at $t_p \approx 10^3$ s). Instrumentally, a dedicated MPR spectrometer could be designed with respect to increased neutron detection efficiency and proton momentum bite as well as improved background handling capability; the latter is needed to measure lower AKN/DTN values than now. All considered, a 1.5-GW plasma on ITER could be observed giving $2 \cdot 10^5$ counts in the AKN region of observation and the covered energy range could be increased so as to approach the predicted upper limit of the AKN spectrum ($E_n \approx 20$ MeV).

The most direct information from AKN measurements concerns the α-particle pressure [7] whose variation would be reflected in the AKN/DTN ratio. This α-particle information is indirect as it is derived with the help of plasma model calculations of the kind presented here. For instance, the AKN emission can be used to prove or disprove a classical fast α-particle source function. Finally, a precipitous drop in the AKN amplitude could be detected with a time resolution of the order ms on ITER. Should such fast changes occur, they would reflect a sudden loss of confinement of the fast d' and t' populations, while loss of fast α's would appear smoothed and delayed over time on the time scale of τ_α.

In conclusion, we have reported the first observation of the α-particle knock-on (AKN) neutron emission from magnetically confined DT fusion plasmas of JET. The α-particle signal is a conspicuous feature of the measured spectrum whose magnitude and electron temperature dependence were found to agree with theoretical predictions based on collisional (classical) α-particle slowing down with nearly 100% confinement. The magnetic proton recoil spectrometer used at JET can be further developed for use on a magnetically confined burning fusion plasma to carry out measurements with 10^4 higher statistics. Neutron emission spectrometry deserves consideration as a burning plasma α-particle diagnostic based on the projected performance of the successful test presented.

This work was carried out under the EURATOM-NFR and the EURATOM-ENEA-CNR association agreements, with financial support from NFR, CNR, and EURATOM. The JET team is gratefully acknowledged for reaching the record DT fusion plasmas making this experiment possible.

[1] B. C. Stratton *et al.,* Rev. Sci. Instrum. **68**, 269 (1997).
[2] R. K. Fisher *et al.,* Phys. Rev. Lett. **75**, 846 (1995).
[3] J. Källne and G. Gorini, Fusion Technol. **25**, 341 (1994).
[4] R. K. Fisher, P. B. Parks, J. M. McChesney, and M. N. Rosenbluth, Nucl. Fusion **34**, 1291 (1994).
[5] G. Gorini, L. Ballabio, and J. Källne, Rev. Sci. Instrum. **66**, 936 (1995).
[6] R. K. Fisher, P. B. Parks, J. M. McChesney, and M. N. Rosenbluth, Rev. Sci. Instrum. **66**, 949 (1995).
[7] L. Ballabio, G. Gorini, and J. Källne, Phys. Rev. E **55**, 3358 (1997).
[8] M. Keilhacker *et al.,* Nucl. Fusion **39**, 209 (1999).
[9] J. Källne *et al.,* Rev. Sci. Instrum. **70**, 1181 (1999).
[10] H. Henriksson *et al.* (private communication).
[11] L. Ballabio *et al.,* Nucl. Fusion **40**, 21 (2000).
[12] J. Frenje *et al.,* Rev. Sci. Instrum. **70**, 1176 (1999).
[13] P. R. Thomas *et al.,* Phys. Rev. Lett. **80**, 5548 (1998).
[14] W. Heidbrink and G. J. Sadler, Nucl. Fusion **34**, 535 (1994).
[15] Y. Shimomura *et al.,* Nucl. Fusion **39**, 1295 (1999).